Channel wall effects in radiation-diffraction analysis

J. N. Newman
jnn@mit.edu

(Submitted to the 31st IWWWFB – Plymouth, MI, USA – 3-6 April 2016)

1 Introduction

Computations of wave-body interactions are usually performed for an unbounded horizontal domain, whereas experiments are performed in tanks of finite width. Reflections from the tank walls can be significant if the width is of the same order as the body length or wavelength, especially when the forward speed of the body is small or zero. In the numerical approach based on linear potential theory using the usual free-surface Green function, the boundary condition on the walls can be satisfied with an infinite array of image Green functions. However, the convergence of the resulting series is too slow to sum directly. Kashiwagi (1) and Chen (2) replace the infinite series by integral representations which can be evaluated numerically. More efficient expressions have been derived by Linton (3). Xia (4) describes a more direct summation approach for the Green function, which is extended by Shen & Qin (5) to account for partial reflection from the side walls. Newman (6) showed that useful results can be achieved without extending the Green function, by including a finite number of image bodies; practical levels of convergence are achieved with O(10) images, except in the vicinity of critical wavelengths where the wall reflections are resonant.

Three alternative approaches are compared in the present work: (1) using a finite array of image bodies, (2) adding reflecting walls of finite length, and (3) accelerating the convergence of the infinite series of image Green functions. The first two approaches are pragmatic applications of the conventional radiation-diffraction code for an unbounded free surface. The third approach is 'exact', within the limits of computational accuracy, but it requires a modified code.

Computations are shown for the pitch and heave motions of an elongated ship-like body in a channel with dimensions typical of a conventional towing tank. The body, intended to represent a generic FPSO, is shown in Figure 1. The length is 10m, beam 2.2m, and draft 0.6m. The body is on the centerline of the tank, which has a width w=10m and depth 5m. The computations are performed using the radiation-diffraction code WAMIT.

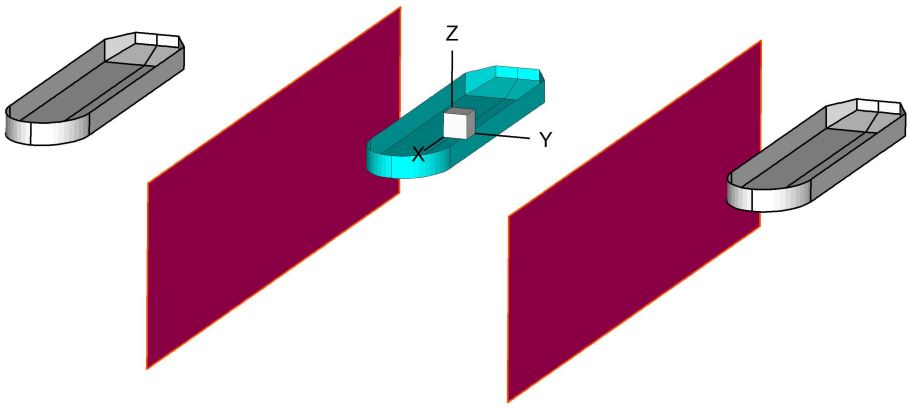

Figure 1: Perspective view of the body (center) with two images, as in the $N = 3$ case used in Section 2, and also showing the $L = 20$ walls used in Section 3.

2 Finite array of image bodies

Three cases are considered with $2, 4, 8$ images, or $N = 3, 5, 9$ identical bodies, equally spaced in the transverse direction with their centerplanes at $y = \pm nw$ ($n = 1, 2, ..., \frac{N-1}{2}$). The radiation force on the middle body is computed with all bodies oscillating with the same amplitude and phase. The heave added-mass and damping coefficients are shown in Figure 2, and compared with the case without walls ($N = 1$) and with the image Green function method (IGF) described in Section 4. The results for $N = 3, 5, 9$ are practically identical for values of the wavenumber k greater than 0.8 or tank widths greater than 1.4 wavelengths. For longer wavelengths the convergence is less satisfactory.

An interesting detail in Figure 2 is the negative damping near $k = 0.5$. This is due to the finite number of images, acting on one body alone, and is not inconsistent with the the fact that the total damping force is positive.

3 Reflecting walls of finite length

In this approach vertical walls of length L are added at $y = \pm\frac{1}{2}w$ as shown in Figure 1, extending from the bottom to the free surface over the longitudinal domain $-\frac{1}{2}L \le x \le \frac{1}{2}L$. The walls are assumed to have zero thickness, and represented by dipole elements to satisfy the condition of zero normal velocity.

The results are shown in Figure 3 for $L = 10, 20, 40$m, and compared with the case without walls ($L = 0$) and with the image Green function method (IGF) described in Section 4. In this case too the convergence is good for larger values of the wavenumber, but for longer waves there are ambiguities which may be attributed to refraction effects from the ends of the walls. The most satisfactory results appear to be for the shortest wall, where relatively good results are achieved for tank widths greater than half a wavelength.

4 Accelerated series of image Green functions

In a channel of width w, with the origin on the centerline, the Green function can be defined formally by the infinite series

$$G^{(C)}(x-\xi, y, \eta, z, \zeta) = \sum_{n=-\infty}^{\infty} G^{(\infty)}(x-\xi, y-(-1)^n\eta - nw, z, \zeta) \tag{1}$$

where $G^{(\infty)}$ is the Green function for an unbounded free surface. This function includes a radiating component, represented in the horizontal plane by the Hankel function $H_0(kR)$ where R is the horizontal distance between the source (ξ, η, ζ) and field (x, y, z) points. The contribution to (1) from this component is evaluated using analytical relations derived by Linton (7). The remaining contribution from the evanescent component of $G^{(\infty)}$ can be summed numerically, since it decays algebraically for infinite depth and exponentially for finite depth when $n \to \infty$.

This procedure is used here, with a modified version of WAMIT. The infinite sum of evanescent components is truncated when the magnitude of the terms is less than 10^{-6}. The results for the heave added-mass and damping coefficients are shown in Figures 2 and 3. The amplitudes of heave and pitch motion are shown in Figure 4.

5 Discussion

Three different schemes are described for computing the forces and motions of a ship-like body in a channel. The results are consistent, except for the anomalies which occur for relatively long wavelengths if the approximate methods described in Sections 2 and 3 are used. The alternative method described in Section 4, based on summation of the image Green functions, is 'exact' and should be accurate within the limits of the convergence tolerances used.

The effect of the walls on the added mass and damping is substantial. In this case, where the body is elongated and the sides are parallel to the channel walls, the principal near-resonances occur when

the distance between the body sides and walls is equal to $n\lambda/2$ where $n = 1, 2, 3, ...$ and $\lambda = 2\pi/k$ is the wavelength. This differs from the case of a more compact body, where the resonant effects occur if the width of the channel is equal to $n\lambda$. In the more exact results based on the image Green function there is some evidence of the latter resonance as well. The heave and pitch amplitudes are not so strongly affected by the walls except very close to the resonant wavelengths.

Substantially more computing time is required to include wall effects in all three methods, especially where a large number of image bodies is used with a corresponding increase in the number of unknowns. In the image Green function method (IGF) the number of unknowns is the same as for the body without walls, but more time is required to evaluate the Green function. In addition it should be noted that a large number of closely-spaced wave frequencies is required to describe the features in Figures 2-4.

References

[1] Kashiwagi, M., 'Radiation and diffraction forces acting on an offshore-structure model in a towing tank,' International Journal of Offshore and Polar Engineering, **21**, (2) 101-7 (199l).

[2] Chen, X., 'On the side wall effects upon bodies of arbitrary geometry in wave tanks,' Applied Ocean Research **16**, 337-345 (1994).

[3] Linton, C.M. 'A new representation for the free-surface channel Green's function,' Applied Ocean Research **21**, 17-25 (1999).

[4] Xia, J. 'Some insight into the Green function of the channel problem,' 17th IWWWFB (2002).

[5] Shen, J. & Qin, H.D. 'Tank Green function with partial reflections from side walls,' 26th IWWWFB (2011).

[6] Newman, J.N. 'Wave effects on multiple bodies,' *Hydrodynamics in Ship and Ocean Engineering,* M. Kashiwagi (ed), RIAM, Kyushu University, 3-26 (2001).

[7] Linton, C.M. 'The Green's function for the two-dimensional Helmholtz equation in periodic domains,' Journal of Engineering Mathematics **33**, 377-402 (1998).

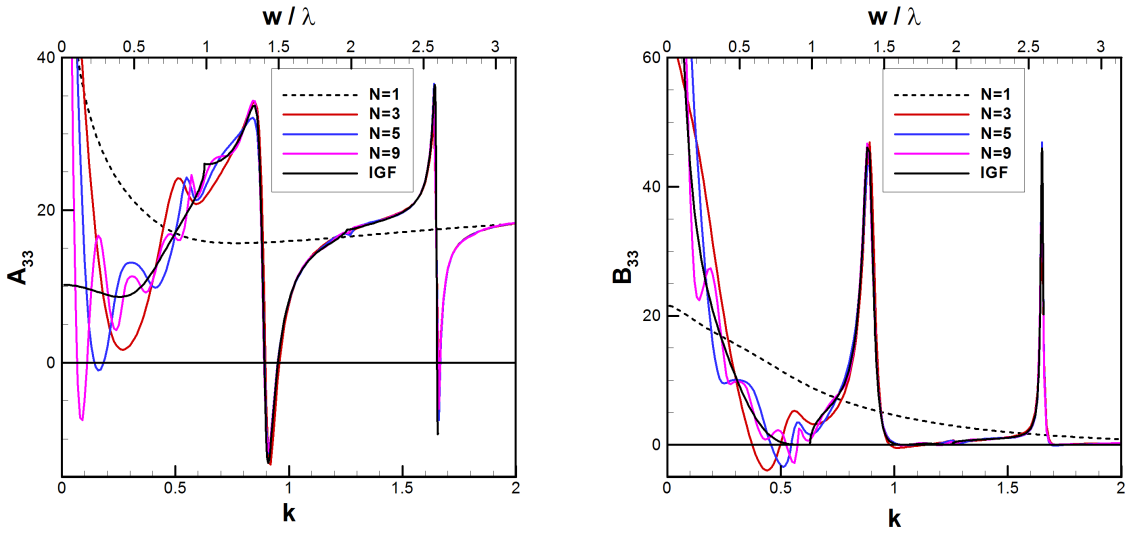

Figure 2: Heave added-mass (A33) and damping (B33) coefficients with $(N-1)$ images. The dashed lines $(N = 1)$ are for the case of one body in an unbounded fluid. The solid colored lines are for $N = 3, 5, 9$ bodies, showing the force acting on the middle body when all of the bodies move with the same amplitude and phase. The black solid lines (IGF) are the 'exact' results based on the method in Section 4.

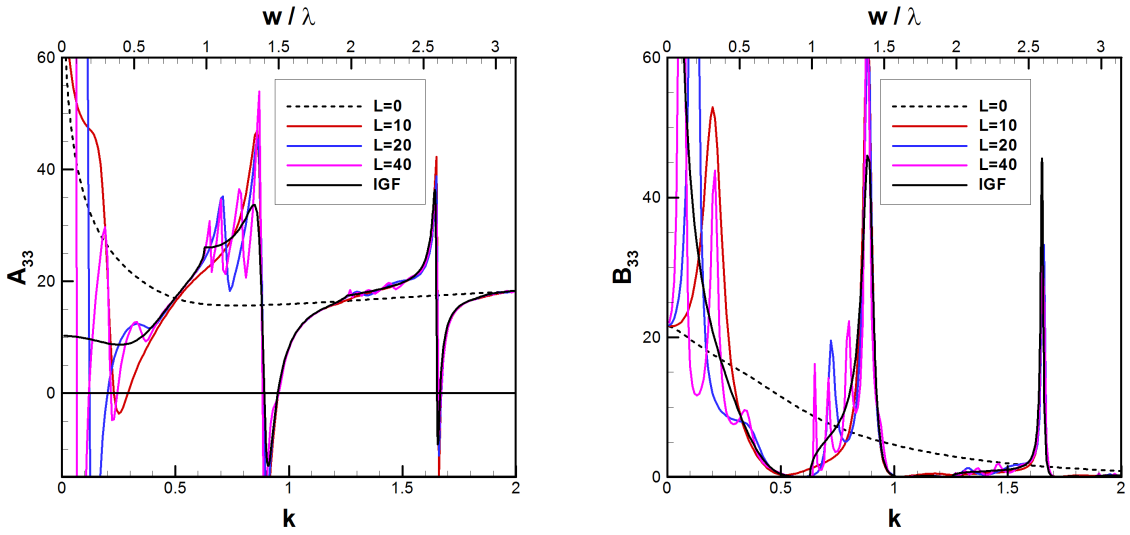

Figure 3: Heave added-mass and damping coefficients of the body between two walls of finite length L. The dashed lines ($L = 0$) are for the case of an unbounded fluid without walls. The solid colored lines are for walls of length $L = 10, 20, 40$. The black solid lines (IGF) are the 'exact' results based on the method in Section 4.

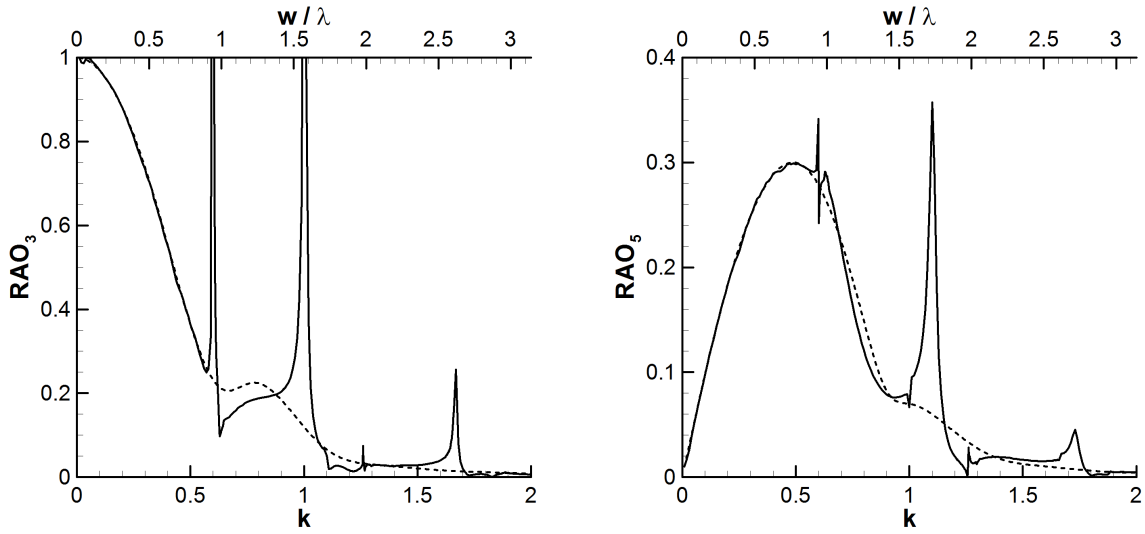

Figure 4: Heave (RAO_3) and pitch (RAO_5) amplitudes of the body between two walls, computed by the accelerated-convergence method described in Section 4. The dashed lines are for the body without walls.